ITT

ITT Industrial Laboratories

a division of International Telephone and Telegraph Corporation
3700 East Pontiac Street, Fort Wayne, Indiana 46803
Telephone (219) 743-7571 TWX 241-2065

ITTIL 66-1037

June 24, 1966

SEVENTH QUARTERLY REPORT

RESEARCH IN THE DEVELOPMENT

EFFORT OF AN IMPROVED

MULTIPLIER PHOTOTUBE

Contract No. NASw 1038

National Aeronautics and Space Administration

Washington, D. C. 20546

Prepared by

F. H. Barr and E. H. Eberhardt

Approved by

S. M. Johnson, Jr., Manager
Advanced Product Development

M. F. Toohig, Manager
Tubes and Sensors Department

Dr. C. W. Steeg, Director
Product Development

INTRODUCTION

Our efforts during this report period have been directed toward three basic problems as follows:

1. An investigation of the counting properties of tubes in which the instantaneous effective cathode diameter (IEPD) has been increased by a new tube design to approximately 0.4 inch to 0.5 inch. These investigations have been undertaken because of the information received as a result of our numerous contacts with astronomical observatories including Lick, Yerkes, Washburn, McDonald and Sydney (Austrailia) Observatories, which have indicated an urgent need for counting photomultiplier tubes of this type.

2. An investigation of the counting properties and increased effective photon counting efficiencies of tubes especially designed for enhancement of the cathode quantum efficiency by means of "multi-bounce" optical techniques. It is clear that improved optical detectors will require a combination of the highest possible cathode quantum efficiency and the best electron counting capabilities, and we have attempted to optimize these properties by incorporating a rectangular effective cathode area (encompassing the multi-bounce areas) in one of our electron counting tubes.

3. Measurements of the pulse response properties of counting tubes. This investigation was instigated because of the expressed need for fast response by astronomers in order to cover as wide a dynamic counting rate range as possible without modifying the detector system, a desirable objective in extracting the maximum amount of stellar information.

1 0 LARGE EFFECTIVE PHOTOCATHODE AREA

The diameter of the effective photocathode of the majority of ITTIL multiplier phototubes is of the order of 0.100 inch, though somewhat larger cathodes may be obtained by proper selection of the aperture diameter. The maximum effective cathode diameter is, of course, set by the diameter of the actual formed photocathode (0.750 inch), though the practical limit may be somewhat less than this. This limit, however, may not be obtained simply by changing the physical aperture diameter because of dynode size limits. In addition, the magnification of the electron optics as well as the area of dynode one must be changed in order to accommodate the larger photocathode diameters.

Presently, a tube having an 0.5 inch effective diameter cathode and a 12-stage multiplier is under development for a NASA customer* and test data on a sampling of these tubes is presented in this report. Figure 1 is a photograph of a typical tube of this type. The image section of these tubes is of the same design as the standard FW Series of multiplier phototubes except for modifications required to produce a magnification of 0.4 instead of the usual value of 0.7, for the reasons mentioned above. The photocathode may be any one of several types formed on the vacuum side of the entrance window which is sealed into the metal cathode sleeve. Connections to the cathode are made by way of this sleeve.

Two methods of cathode processing have been used. In both cases, the channels for evolution of the alkali metals were placed in an external bulb attached to the tube by the tubulation nearest the cathode. In most of these tubes, the antimony evaporator was permanently mounted in the tube, while in one the antimony evaporator was inserted on a retractable member, through the same tubulation so that it could be removed after the evaporation process. This type of evaporation has not produced a satisfactory high sensitivity cathode as yet; however, the tube was operable. This method leaves the tube completely free of processing leads, thus simplifying the internal tube structure.

The multiplier section, as can be seen in Figure 1, is enclosed within a metal sleeve separating the image section and the glass stem, hopefully reducing dark noise. This metal sleeve is also the defining aperture terminal. The cascade aperture and all dynode leads are brought out through a 13 pin stem while the coaxial lead at the center of the stem serves as the anode connection. While this connection is a standard subminiature 50 ohm connector, no attempt as yet has been made to maintain this ultra-low impedance, configuration inside the tube. The load impedance used in most of the tests is of the order of 10^5 or 10^6 ohms.

---

* University of California, Lick Observatory NASA Prime Contract 05-003-100-1 (Subcontract to ITTIL, G607170).

Performance characteristics of this tube include the ability to count single events at the cathode as well as improved rise and transmit times, compared to the standard line of ITTIL multiplier phototubes.

1.1 Cathode Characteristics

The four tubes which are reported on here have S-20 type cathodes on a sapphire window. Tubes of this same design but with S-11 cathodes are also being built but prototypes were not available for final test at this writing. The spectral response of these four cathodes is shown by the solid line in the plot of Figure 2, while the dashed curve is the typical response of an S-20 surface formed on a visible light transmitting window* such as 7056 glass which is normally used in this laboratory. The short wavelength limit of the solid curve is set by our present means of measuring this parameter, namely a calibrated tungsten 2870 degrees K lamp and a set of Optics Technology narrow bandpass filters. At present, a McPherson model 235 Vacuum UV Monochrometer is being readied for operation which will permit measurements of this type to be made down to 1000 angstroms. It is safe to predict, however, that the response of these cathodes should have the same general shape below 4000 angstroms as the S-13 surface (Cs-Sb on fused silica) which has extended ultraviolet response due to the transmission of the window material.

In order to determine the effective photocathode size and the response uniformity, the photocathode was mechanically scanned with a small spot of light while the output of the multiplier was monitored with a d-c oscilloscope. Figures 3 and 4 show the plots of this data as a function of displacement along two mutually orthogonal diameters, one of which is parallel to dynode one.

The curves marked (a) are plots from left to right along the length of dynode one and those marked (b) are plots from the open side, toward dynode two, to the back of dynode one. It should be remembered that, the electron lens produces an inverted image so that nonuniformities on the one side of the cathode are superimposed on nonuniformities on the opposite but corresponding side of dynode one. The gross nonuniformities of the output signal are for this reason, a composite of opposite halves of cathode and dynode one. It has been shown, however, in an earlier report on this project** that the cathode shading in general is not nearly pronounced enough to account for the total output signal shading but that the gain of dynodes one and the collection efficiency for dynode two account for the largest portion of this effect.

---

* Typical Absolute Spectral Response Characteristics of Photoemissive Devices, ITTIL Wall Chart.

** Third Quarterly Report NASw 1038 May 28, 1965.

This data shows clearly, however, that the effective cathode dimensions are about 0.6 by 0.5 inch when measured at the half amplitude points of these curves. The downward deflection of the scope trace, for maximum signal, is due to the negative going voltage produced across the load resistor by the output current.

1.2 Multiplier Response Time Characteristics

Aside from the usual electron multiplier characteristics, such as gain, dark current, ENI, etc., the single pulse transit time is of particular interest since this tube is to be used to detect signals which range from those able to excite only single electrons from the photocathode to those of such intensity as would produce a dc anode output due to pulse overlap.

Figure 5 is a block diagram of the special test equipment used by ITTIL to make the required response time measurements. It consists essentially of a high speed triggered light source which illuminates the multiplier under test, and a photodiode. The output signals from these tubes are fed to a dual trace sampling scope whose time base is also triggered by the light source. Since this process is controlled by a trigger generator at a regular occurring rate, the scope presentation shows these events in their proper time relationship.

Figure 6 shows these scope presentations for the specified operating conditions. In Figure 6a, the tube is operated as indicated with the cascade aperture (A_2) connected to dynode one and the defining aperture. The larger negative going trace is the multiplier output and the photodiode output is the sharp spike at the left side of the photograph.

The time separation between these two signals is the transit time of the multiplier tube and is approximately 40 nanoseconds with a rise time of 10 nanoseconds, a fall time of 30 nanoseconds and a full width at half the maximum amplitude (FWHM) of about 28 nanoseconds. Figure 6b shows virtually the same results with the cascade aperture (A_2) at -45 volts with respect to dynode one and defining aperture. However, in Figure 6c, when the cascade aperture is again at dynode one defining aperture potential but with increased image section voltage and constant multiplier voltage (to maintain constant gain), the transit time is 30 nanoseconds. In all cases, the rise time (10 to 90 percent) is 10 nanoseconds. The voltage distribution in (c) is typical of the conditions under which the tube is pulse counted though the over-all voltage is somewhat higher than required. The test light pulses are so short (approximately 1 nanosecond, FWHM) that the output current pulses from the tube are essentially identical to those generated by single electron events, but with much larger, more easily observable magnitudes.

In the foregoing test, the rather high operating voltage is required in order to develop the necessary output voltage across the 50 ohm load impedance.

With the above information and a knowledge of other conditions such as multiplier gain, pulse processing methods and tolerable number of lost pulses, a calculation can be made as to the maximum permissible dc output current which will keep the pulse rate just below the time resolution limit of the phototube.

1.3 Pulse Amplitude Distribution Characteristics

Figures 7 through 10 are the single electron spectra of these tubes with their respective dark noise spectra. In all cases the cascade aperture was operated at a potential of -30 to -45 volts with respect to dynode one and the defining aperture. In Figure 7, tube number 046603 shows a markedly lower dark count than the other three, though the dark spectrum does show the same general shape as the signal spectrum. The other three tubes have much higher dark count and the distribution is just like that of the signal spectrum.

If, however, the cathode is biased off to dynode two potential, these dark pulses are almost entirely eliminated and are not shown on the plots.

This fact is taken to indicate that these tubes would cool well, and in fact, a communication from the customer at this writing reports a dark counting rate of a few counts per second, is dry ice temperatures, for one tube.

A recurring problem in these tubes has been the presence of large pulses not associated with the signal input to the photocathode. A preliminary test of a tube like the ones just described (but with an S-11 type cathode) showed poor statistics with the cathode excited in the usual manner and the single electron peak could only be resolved when the dark count was subtracted. An inspection of the scope monitoring the input pulses to the analyzer showed that many large pulses were also present. It was also observed that the number of these pulses varied with the image section voltage. In order to investigate this effect the analyzer was adjusted so that it counted pulses whose amplitude fell within the region from channel 50 to 150. Since the single section peak was centered about channel 15, pulses falling in channels 50 to 150 represent pulses of from 5 to 10 electrons. Figure 11 shows the total number of pulses in this region plotted against the voltage applied across the image section. During these tests the voltage across the multiplier was held constant in order that the overall gain of the system did not change. This seems to be a clear indication that the source of these larger pulses is in the image section.

Two other parameters of interest for these tubes are shown in Figures 12 and 13, namely anode responsitivity and dark current.

Inspection of these two curves shows that at a gain of 10^6 the dark current ranges from 1 to 2.5 nanoamperes. Tube number 046603 had very unusual dark noise characteristics which certainly must contribute to that fact that it has the highest dark current of the four. Figure 14 is a series of three photographs of the output of the pulse preamplifier due to this noise. Careful examination of this tube during operation at 2500 volts, located electrical discharge visible to the dark adapted eye, in the region of the stem leads. However, the cathode was biased to dynode two so that the possibility of optical feedback to the cathode is ruled out. At lower voltages the noise persisted but was not visible. These results indicate that the noise was coupled to the tube output by direct stem leakage.

2.0 TUBES WITH HIGH QUANTUM EFFICIENCY, MULTI-PASS CATHODES

In the last year or two much interest has been shown in ways to improve the quantum efficiency of multiplier phototubes. In this laboratory, first efforts have been directed toward more efficient use of the incoming radiation at the photocathode. *

In the application of a phototube, with a translucent cathode, the radiation enters the cathode at normal incidence. However, a number of events occur which serve to reduce the effectiveness of the input signal.

First of all, some of the input radiation is reflected at the air-glass surface of the faceplate. At the glass-photocathode interface, another reflection occurs while some radiation interacts with the photocathode to produce the desired photoelectrons. Finally, a large fraction of the incident radiation is transmitted into the vacuum space and scattered by reflection off the internal structure of the tube. If the radiation could be made to interact more often with the photocathode, a higher photoelectron yield could be achieved. Figure 15 shows an arrangement which has been tried here with encouraging results. It consists of a prism affixed to the faceplate of the tube. The incoming flux is injected into the faceplate at the critical angle so that it is trapped between the two surfaces and as a result multiple reflections occur causing photoelectrons to be emitted each time the light passes into the cathode layer. Of course, some of the above mentioned losses still occur but it will be shown that the desired effect, namely higher photoelectric yield, due to multiple interaction of the light with the photocathode does, in fact, occur.

---

* J. L. Gumnick & C. L. Hollish - Multiple Reflection Effects Observed for S-1, S-11, and S-20 photocathodes, 10th Scintillation & Semiconductor Counter Symposium, March 2-4 1966, Washington, D. C.

A multiplier phototube having an S-20 slit shaped cathode with an effective size of 0.750 inch by 0.080 inch, was built for a NASA user on another contract. The prism was cemented to the faceplate, with Eastman 910 adhesive so that the path of the multiple reflection could be made to coincide with the slit cathode.

Figure 16 shows two spectral response curves for this tube. One is taken with the input radiation flooding the cathode and the other is taken with the input radiation injected through the prism in such a way that the multiple reflections are visible.

In the first case, the luminous sensitivity was measured to be 105 μa per lumen and in the second case it was 230 μa per lumen. The region of peak sensitivity appears to have shifted about 400 angstroms but the radiant sensitivity is nearly 0.028 ampere per watt higher for the multiple reflection case. An attempt was made to measure the improvement in the anode sensitivity due to this effect. It was discovered that the angle of incidence of the light on the face of the prism is very critical. It appears that normal incidence of the light on the prism face is not a sufficient condition to assure multiple reflections. For this reason it will be necessary to modify the test equipment to provide the needed freedom and accuracy of adjustment to get this data. In actuality, the anode sensitivity measurements were nearly identical for the two modes of operation. Figure 17 is the plot of this data for normal incidence on the photocathode.

The single electron spectra of this tube for the two modes of operation is shown in Figure 18. The tube was operated at 1800 volts with dynode one at -30 volts with respect to the aperture electrode, and the light was injected into the prism with a flexible fiber optic light guide. In this tube, -30 volts on dynode one produced the same results, as far as the pulse height distribution is concerned; as does a negative potential on the cascade aperture in tubes reported previously. This may be due, in part, to the fact that the slit aperture confines the primary electrons to a long narrow area at the center of the dynode where dynode-one bypassing is less likely. A more probable explanation of the observed improvement is the fact that the secondary electron collection efficiency is more uniform for an aperture of this shape. It is obvious, from the two upper curves, that the injection of the signal through the prism does not in any way destroy the tubes ability to detect single events at the cathode. The peak-to-valley ratio for these two conditions of operation remains at 1.65. The slight difference in the peak height is due to the inability to exactly duplicate the light level. Here again, as in the case of the responsivity measurements, there is difficulty in assuring that multiple reflections do in fact occur since the level of illumination is so low as to be inperceptible, and more accurate methods will have to be devised to adjust the angle of incidence at higher light levels in order to visually optimize the reflections.

The dark count is almost entirely cathode originated as can be seen by the shape of the distribution curves. If the cathode is biased off to dynode two potential, there is further evidence of the origin of the dark noise for now the dark count is down to less than two counts per second. As well as being few in number, these counts are located in the early channels of the spectrum where they would not add appreciable error to the detection of pulses of the most probable amplitude.

3.0 FUTURE PLANS

An effort will be made to resolve the difficulties in test equipment so that a quantitative measurement can be made of the increased anode responsivity due to multiple internal reflection in the photocathode.

Two tubes are now being built and processed with attached ion pumps and Baird-Alpert ion gauges to investigate the role of temperature and gas pressure on the noise statistics of these multiplier tubes which was originally reported in the fifth quarter.

A recent innovation in the configuration of dynode one in magnetically focused multiplier tubes, has been investigated briefly in this laboratory. It appears to have a marked effect on secondary electron collection efficiency of dynode two, an effect important to the reduction of small pulses. Present plans call for the incorporation of this feature in tubes of the types being evaluated on this contract.

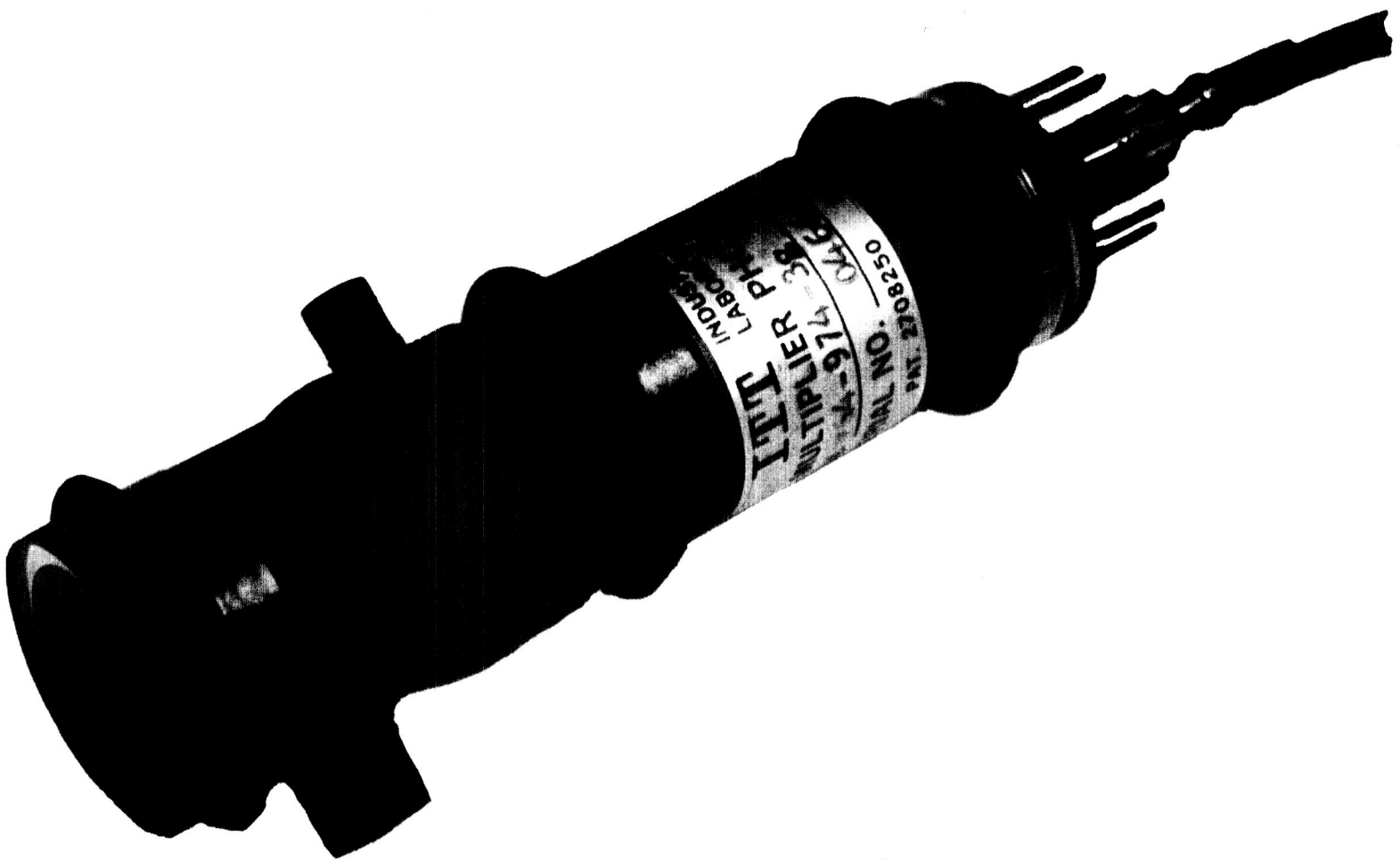

Figure 1

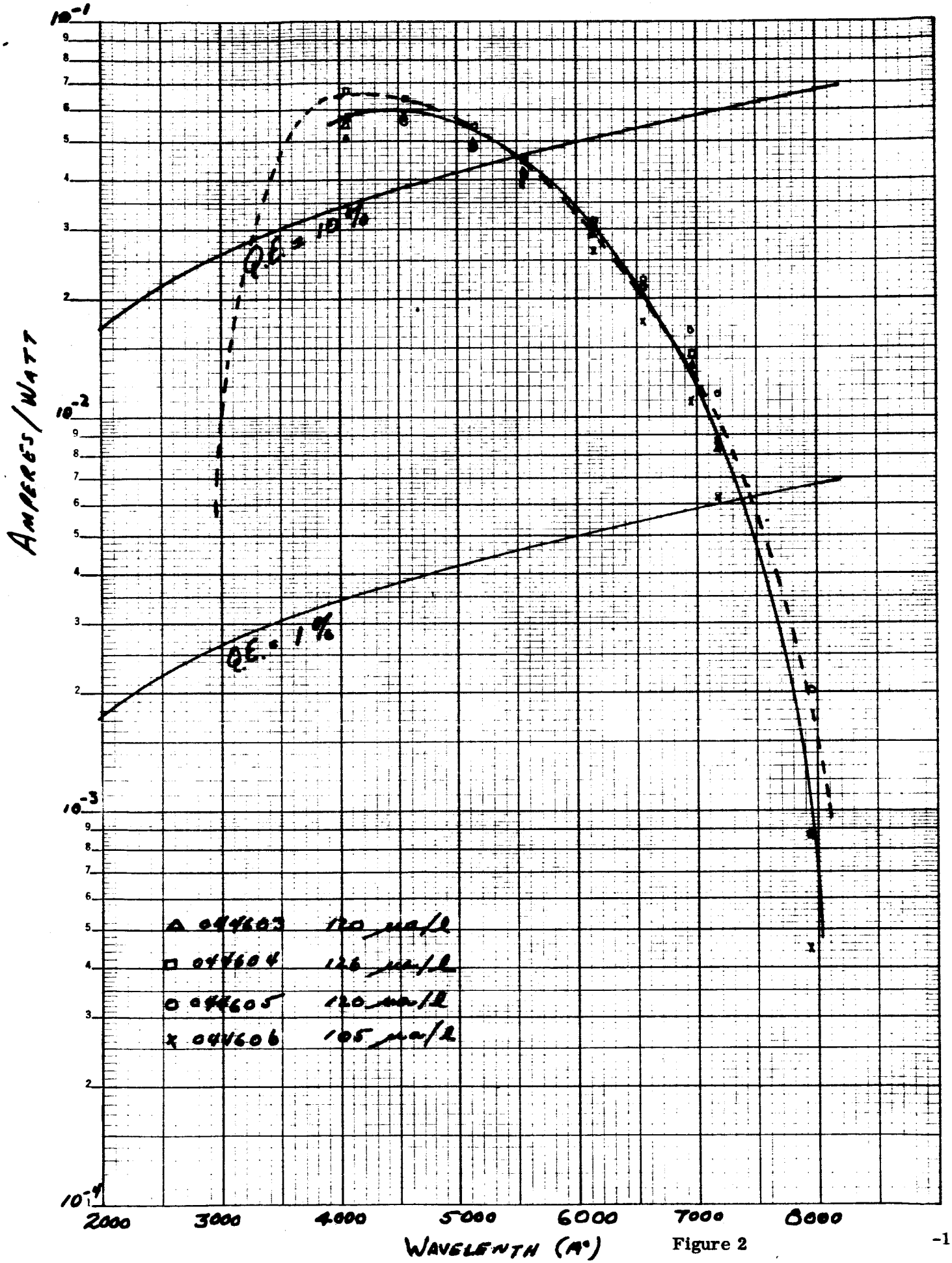
AMPERES/WATT
WAVELENTH (A°)
Q.E. = 10%
Q.E. = 1%
△ 044603 120 μa/l
□ 044604 126 μa/l
○ 044605 120 μa/l
x 044606 105 μa/l

Figure 2

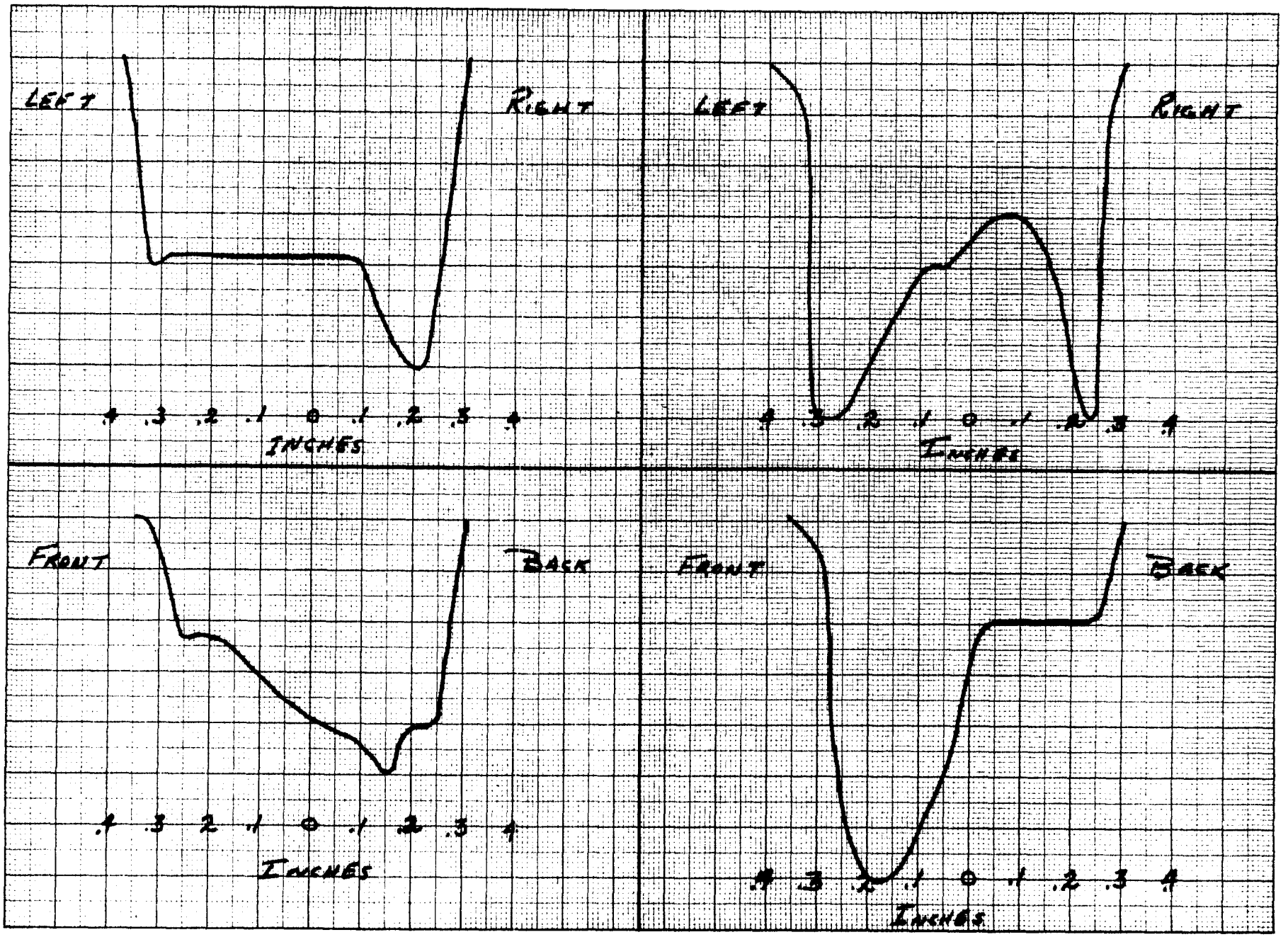

046603

Figure 3

046604

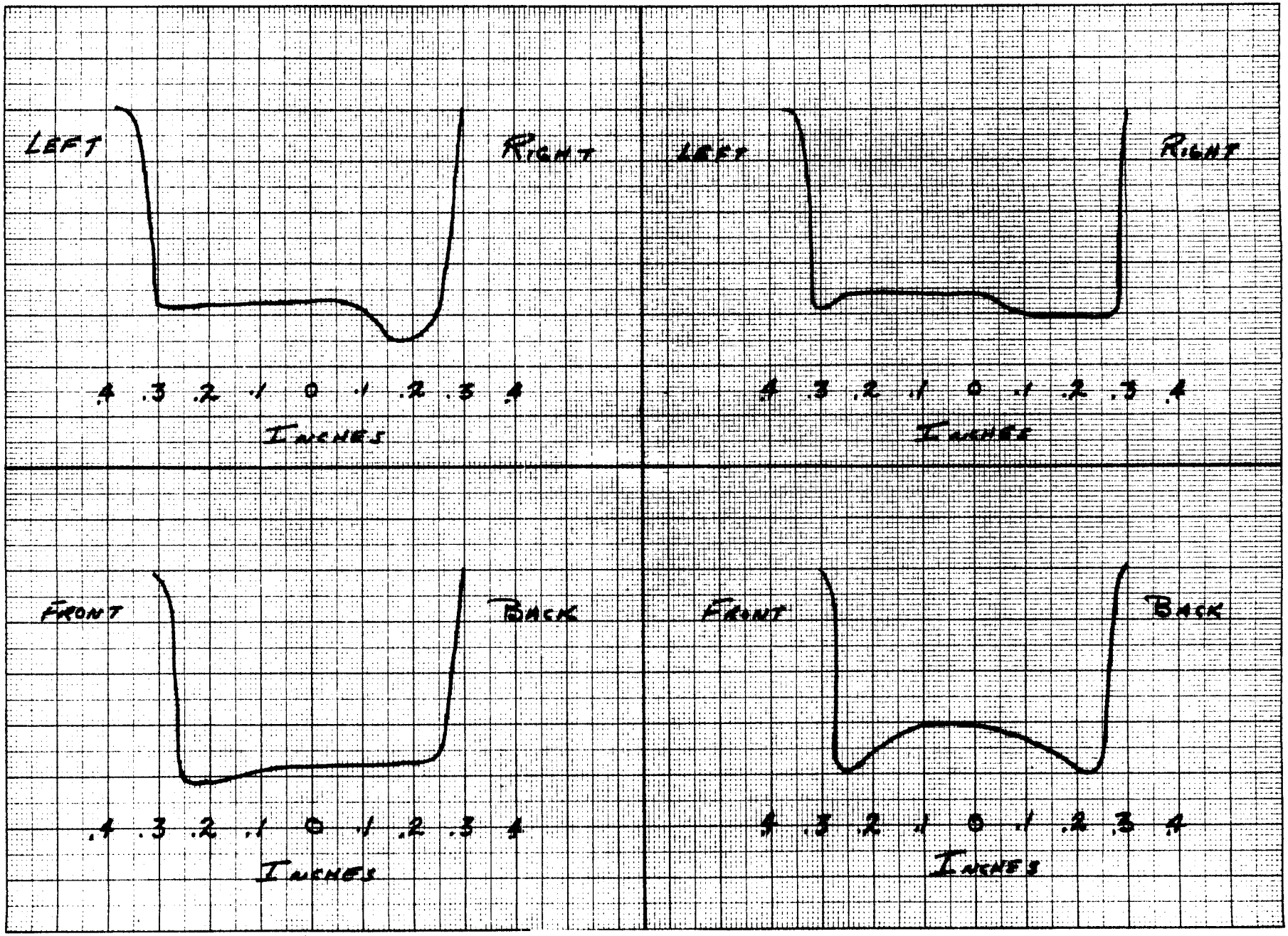

046605

046606

Figure 4

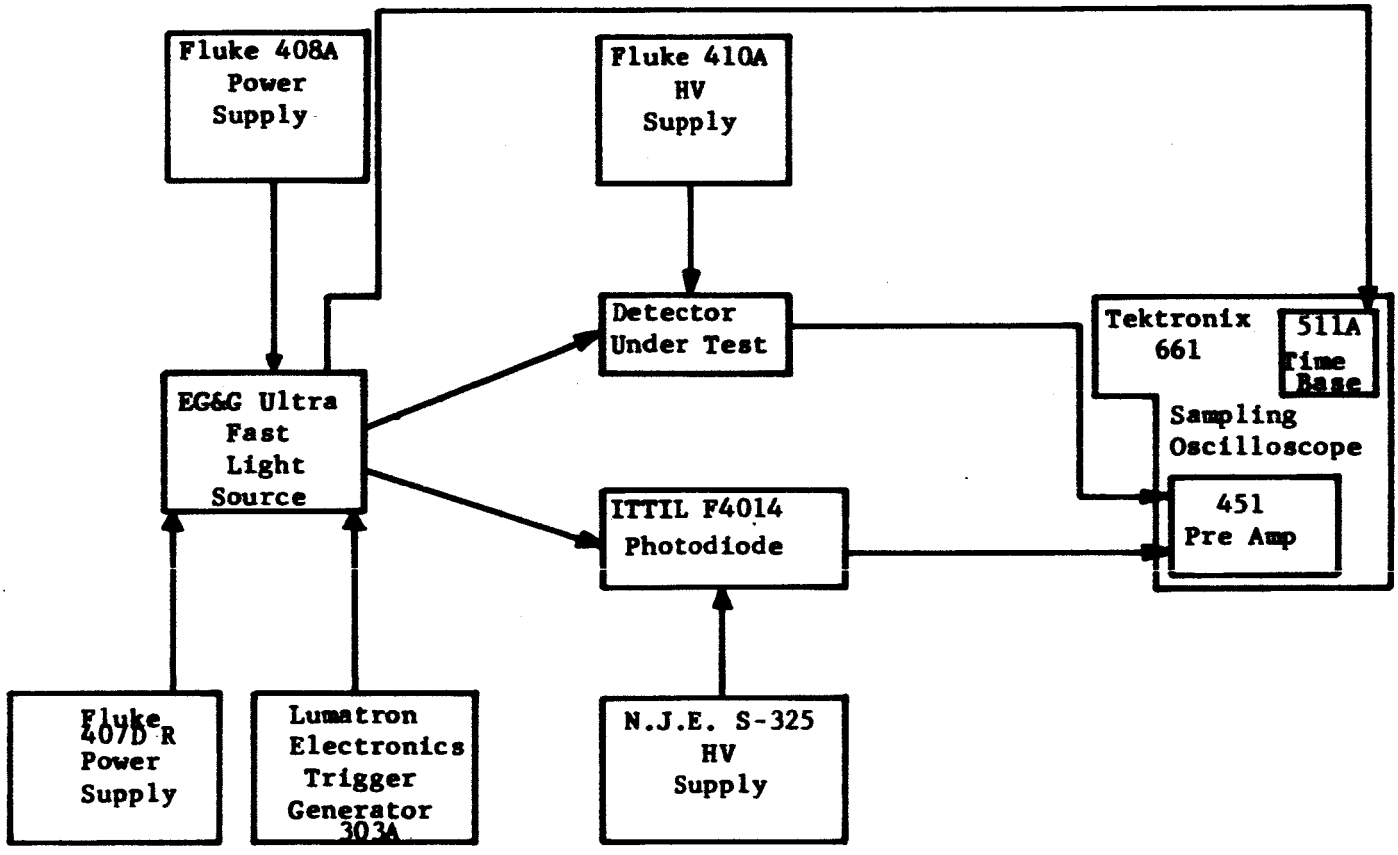
Fluke 408A
Power
Supply
Fluke 410A
HV
Supply
Detector
Under Test
Tektronix
661
511A
Time
Base
Sampling
Oscilloscope
EG&G Ultra
Fast
Light
Source
ITTIL F4014
Photodiode
451
Pre Amp
Fluke
407D R
Power
Supply
Lumatron
Electronics
Trigger
Generator
303A
N.J.E. S-325
HV
Supply

Figure 5

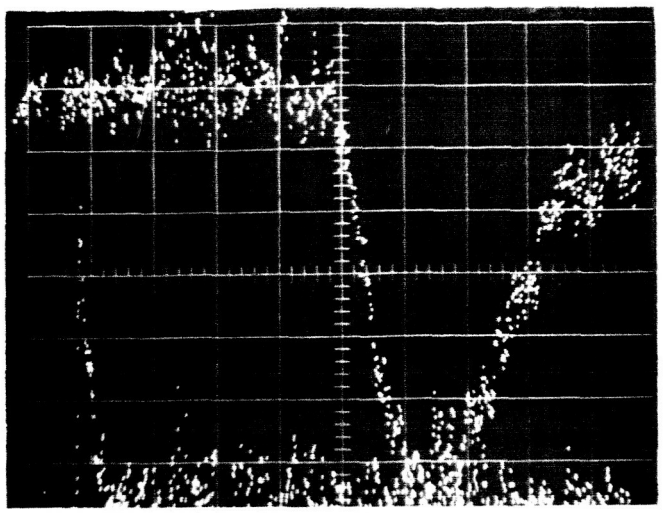

(a) 2000 Volts, 285 Volts Cath-D_1
A_2 at A_1D_1 potential

V = 1 ma/cm
H = 10 nsec/cm

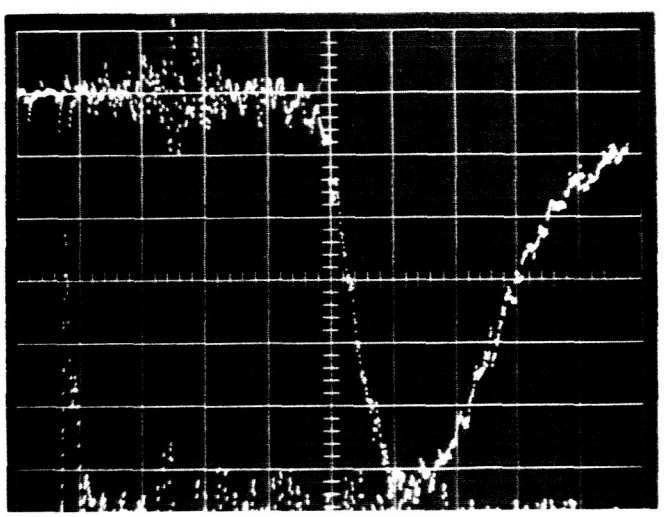

(b) 2000 Volts, 285 Volts Cath to D_1
A_2 -45V with respect to A_1 D_1

V = 1 ma/cm
H = 10 nsec/cm

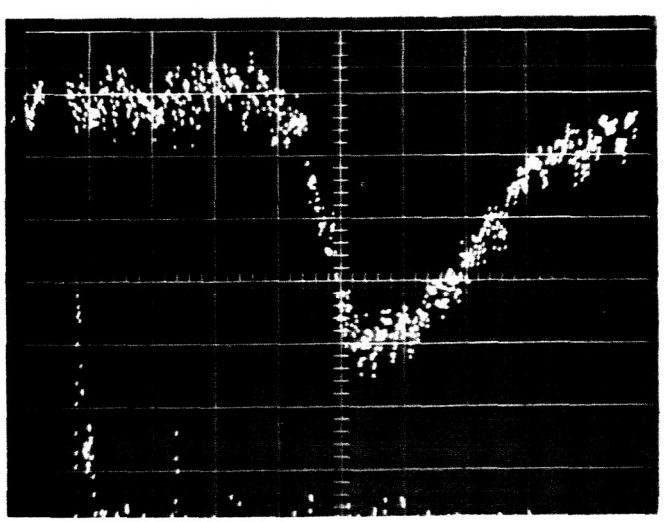

(c) 2600 Volts; 830 Volts Cath to D_1
A_2 at A_1D_1 potential

V = 2 ma/cm
H = 10 nsec/cm

Figure 6

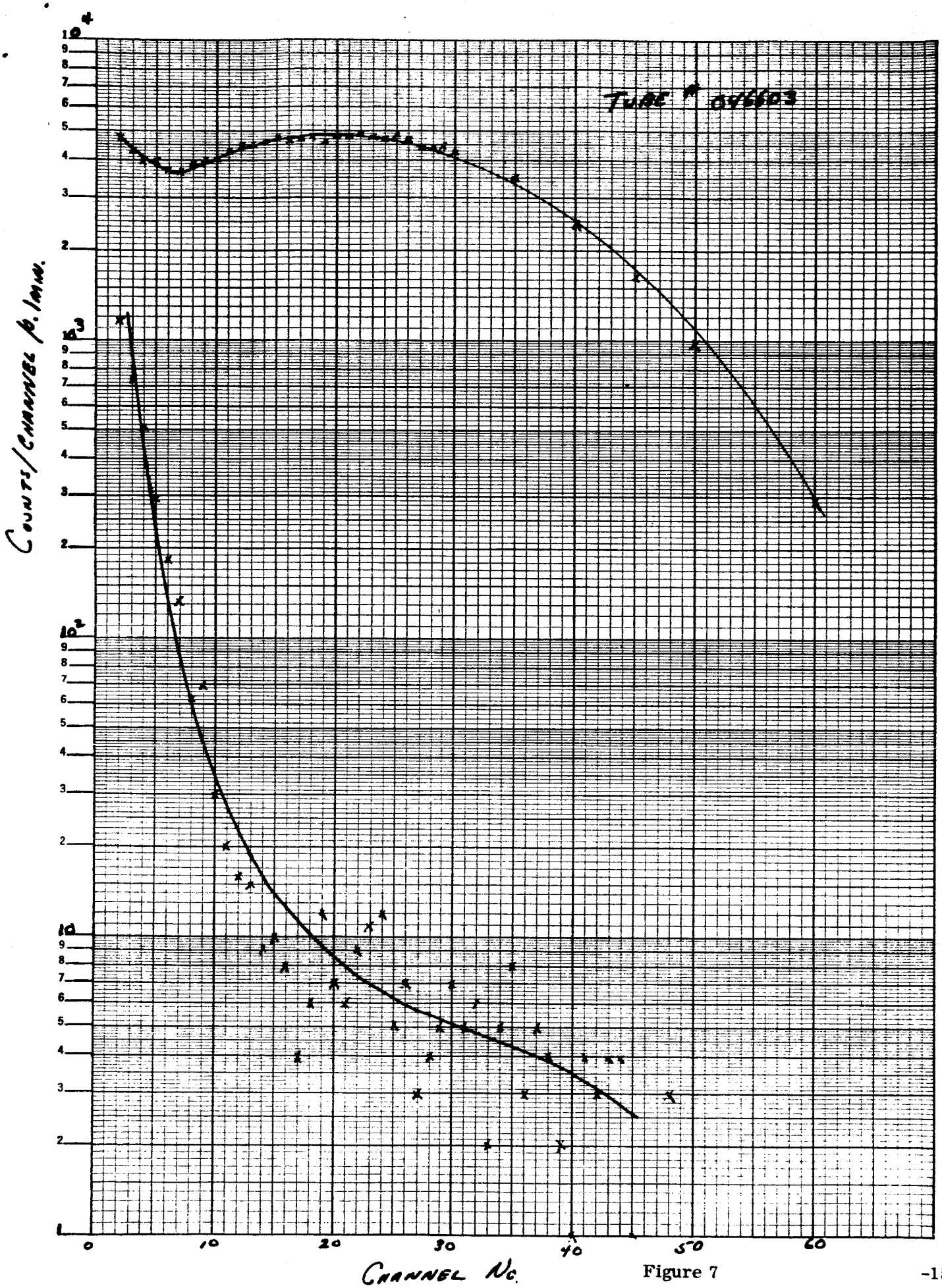
TUBE # 046603
COUNTS/CHANNEL PER 1 MIN.
CHANNEL NO.
0
10
20
30
40
50
60

Figure 7

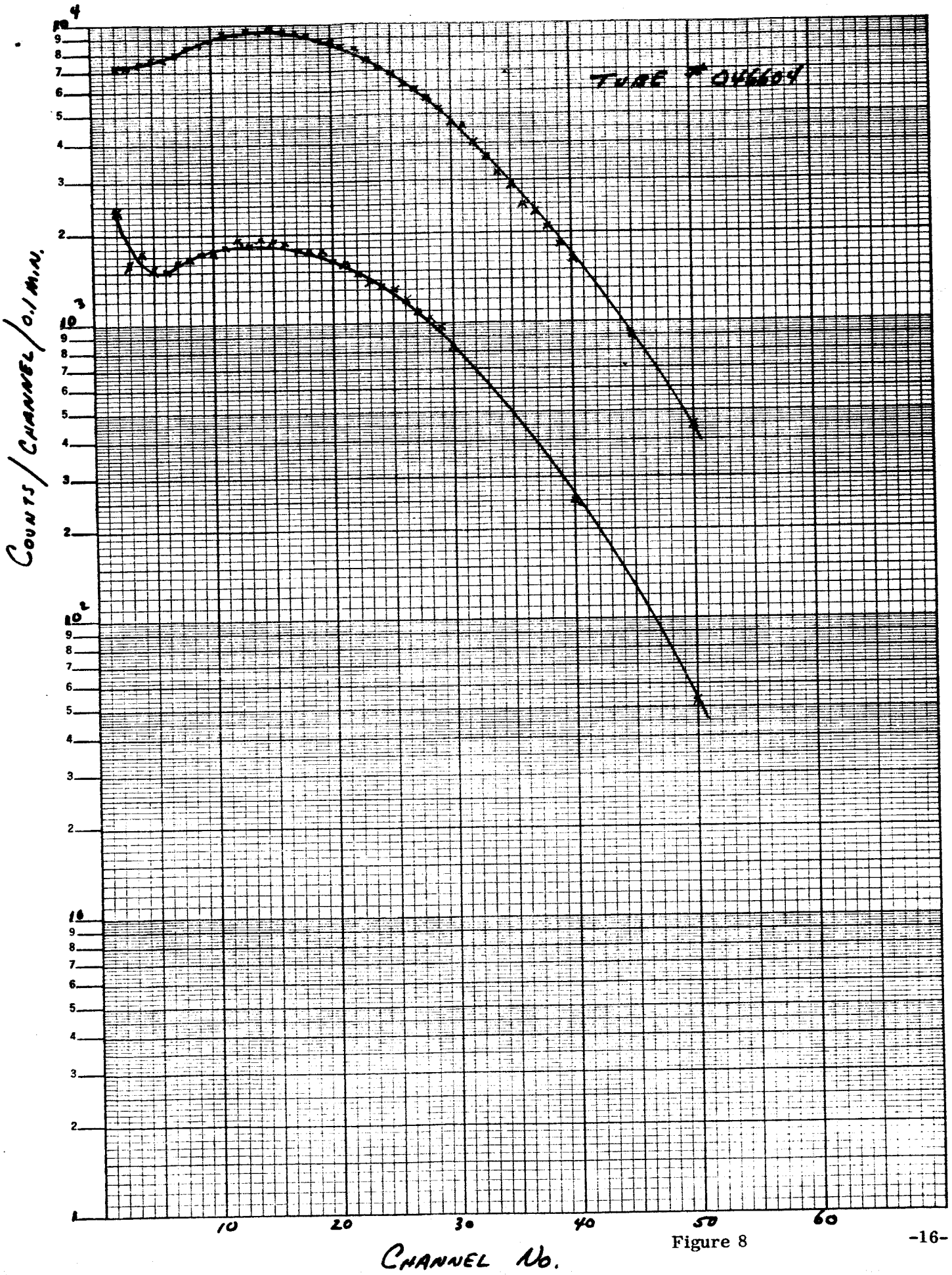
TUBE # 046604
COUNTS / CHANNEL / 0.1 MIN.
CHANNEL No.
10^4
10^3
10^2
10
1
10
20
30
40
50
60

Figure 8

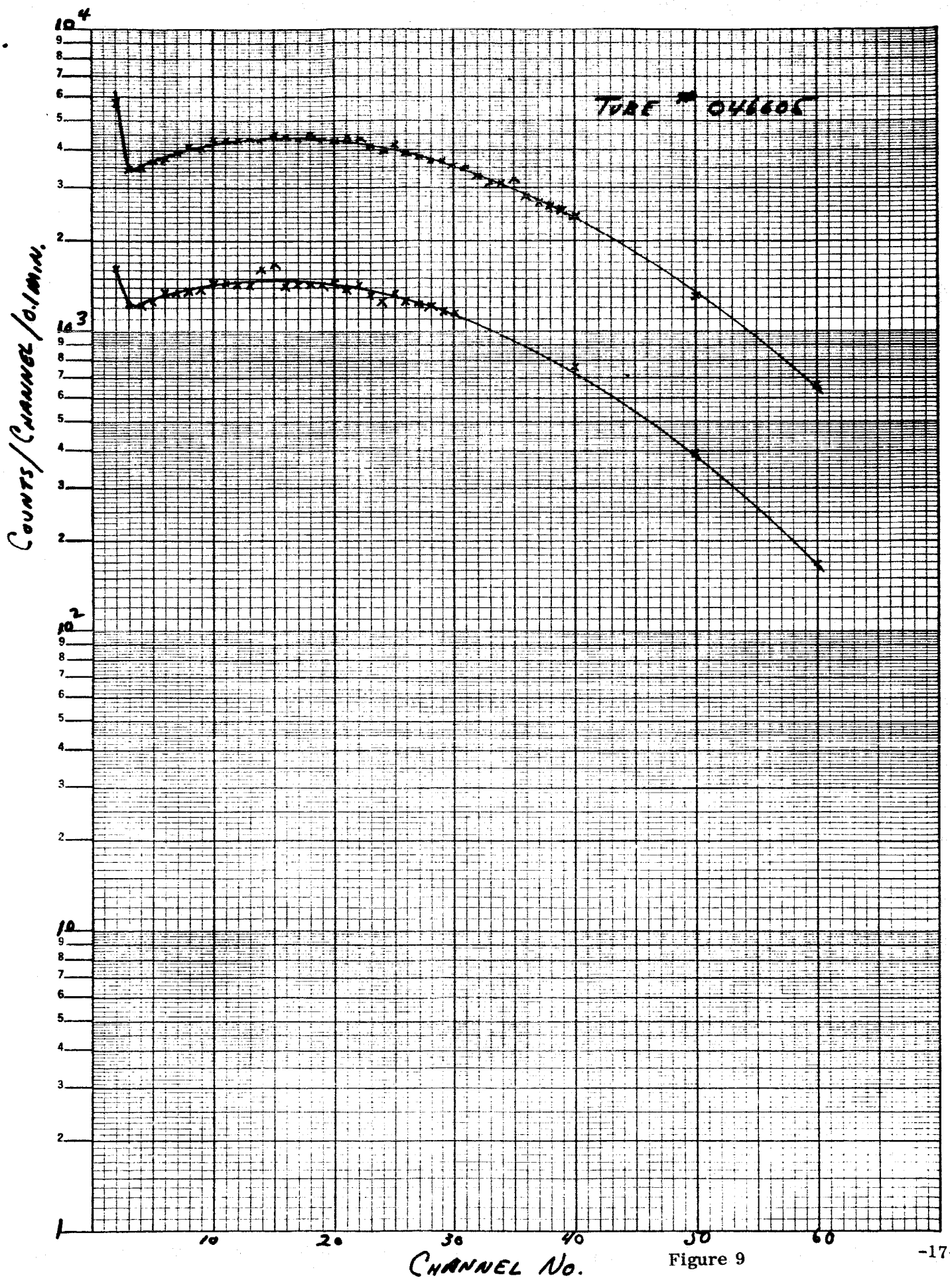
TUBE # 04660C
COUNTS/CHANNEL/0.1MIN.
CHANNEL NO.
10^4
10^3
10^2
10
1
10
20
30
40
50
60

Figure 9

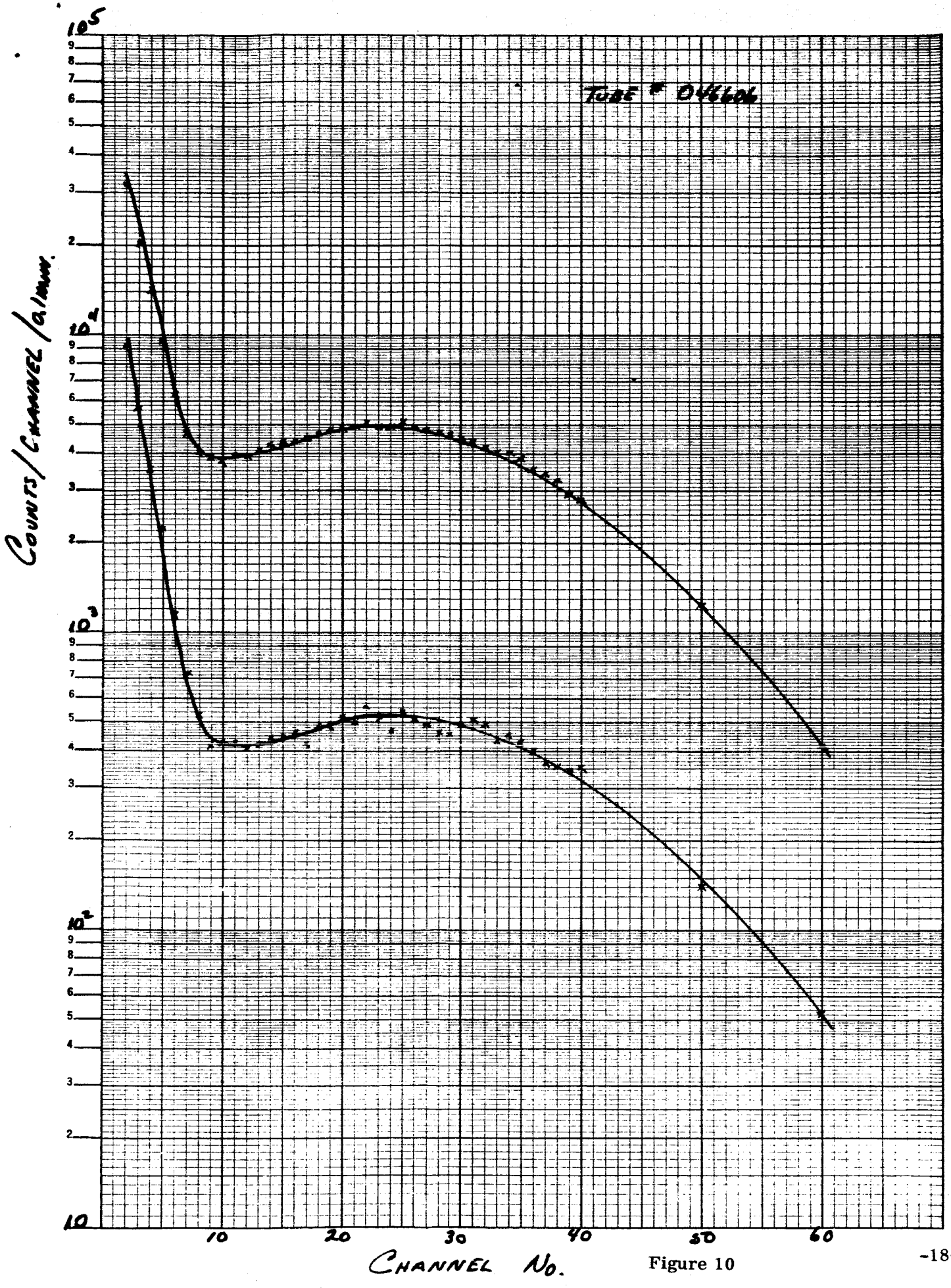
Tube # 046606
Counts / Channel / 0.1 mw.
10^5
10^4
10^3
10^2
10
9
8
7
6
5
4
3
2
10
20
30
40
50
60
Channel No.

Figure 10

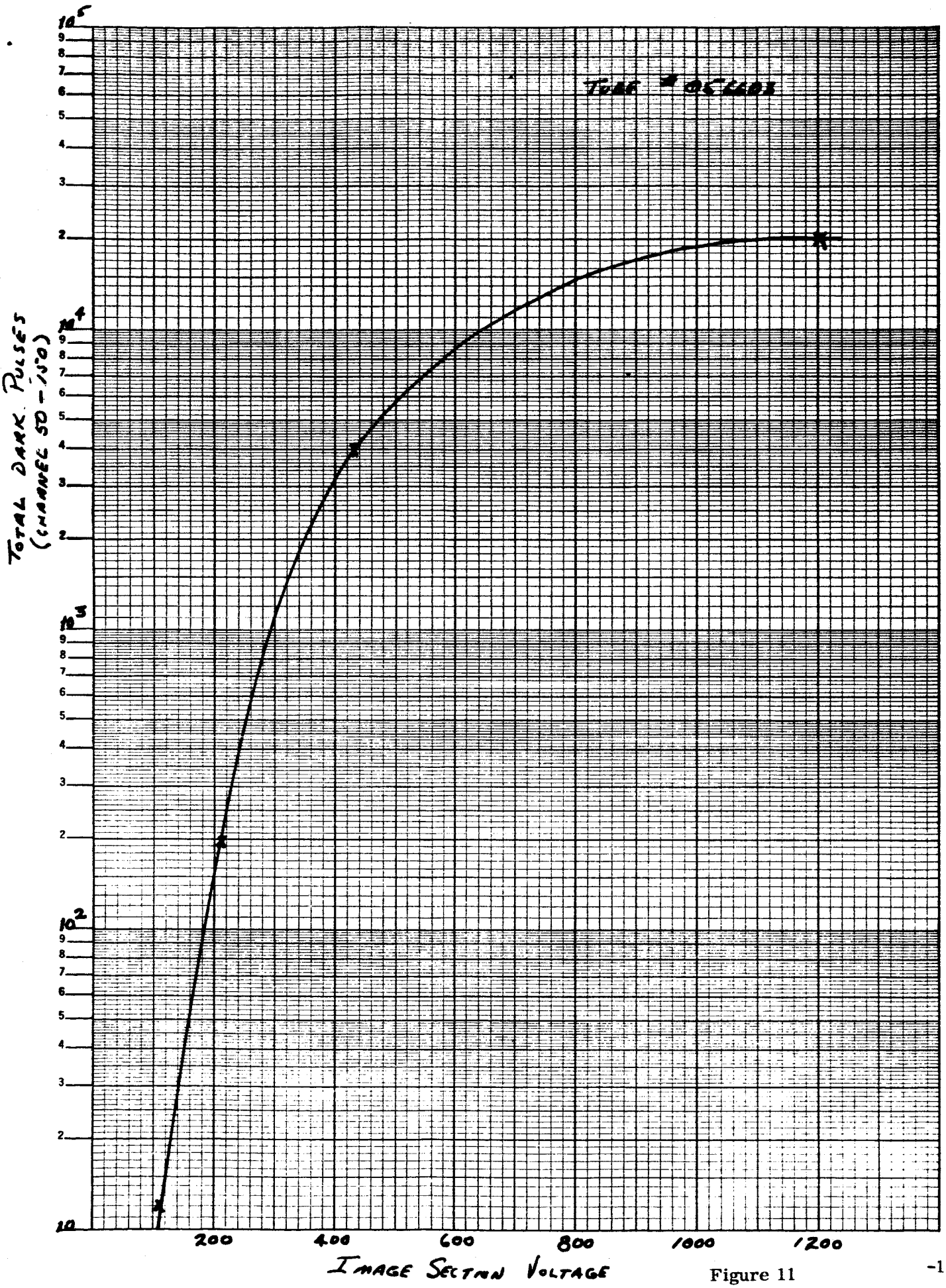
TUBE # 05C6403
TOTAL DARK PULSES (CHANNEL 50 - 150)
10^5
10^4
10^3
10^2
10
200
400
600
800
1000
1200
IMAGE SECTION VOLTAGE

Figure 11

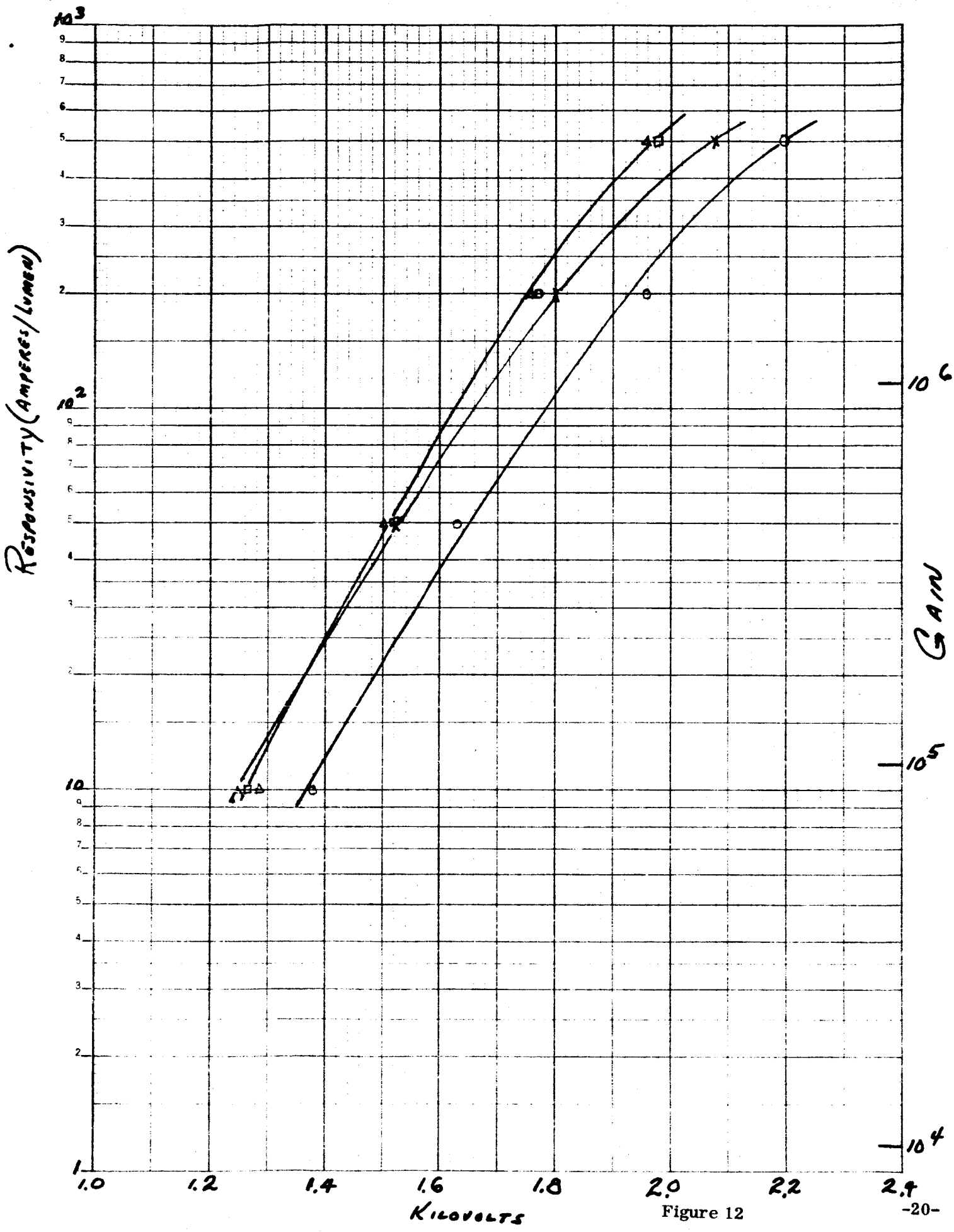
RESPONSIVITY (AMPERES/LUMEN)
10³
9
8
7
6
5
4
3
2
10²
9
8
7
6
5
4
3
2
10
9
8
7
6
5
4
3
2
1
1.0
1.2
1.4
1.6
1.8
2.0
2.2
2.4
KILOVOLTS
10⁶
10⁵
10⁴
GAIN

Figure 12

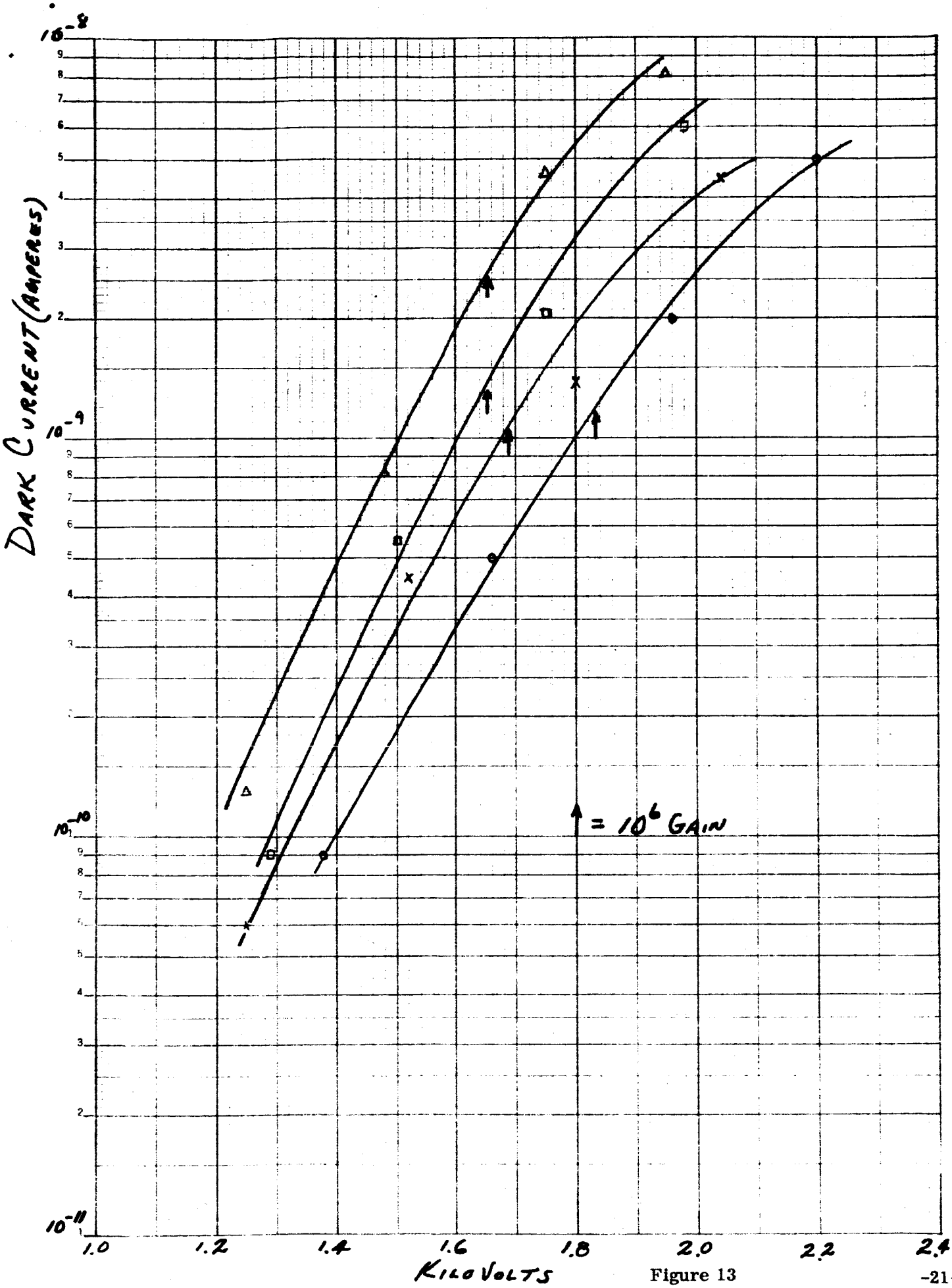
DARK CURRENT (AMPERES)
10^{-8}
10^{-9}
10^{-10}
10^{-11}
1.0
1.2
1.4
1.6
1.8
2.0
2.2
2.4
KILOVOLTS
= 10^6 GAIN

Figure 13

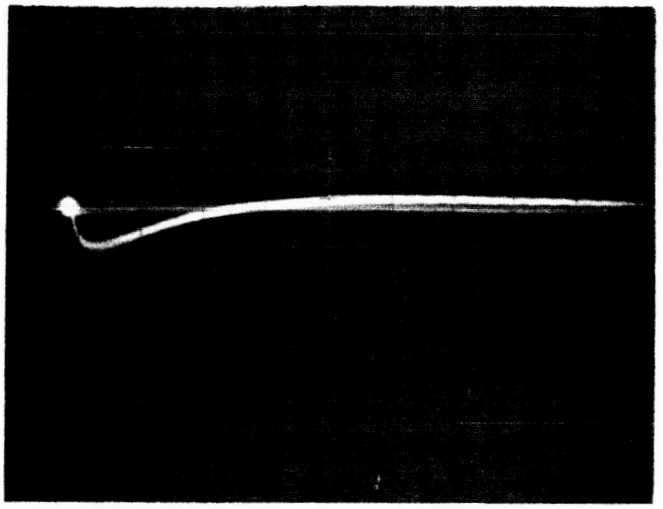

1800 Volts, cathode at D_2 potential

V = 1v/cm
H = 2 μsec/cm

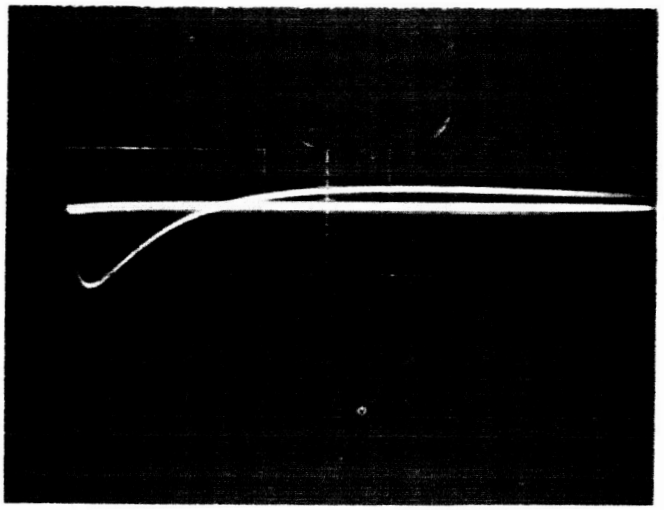

2000 Volts, cathode at D_2

V = 1v/cm
H = 2 μsec/cm

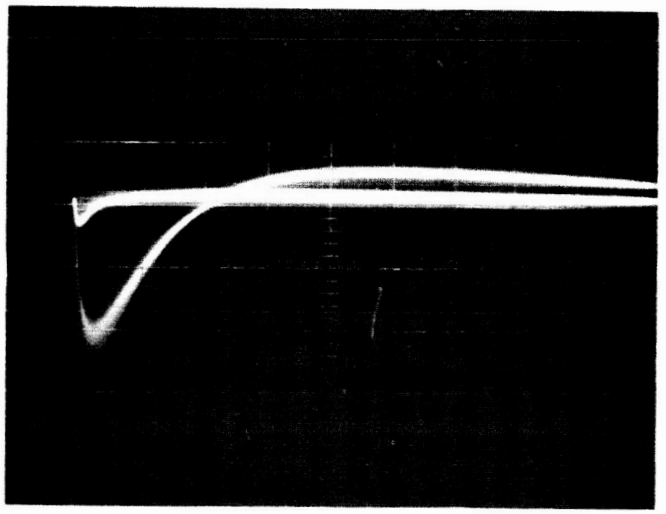

2500 Volts, cathode at D_2

V = 1v/cm
H = 2 μsec/cm

Figure 14

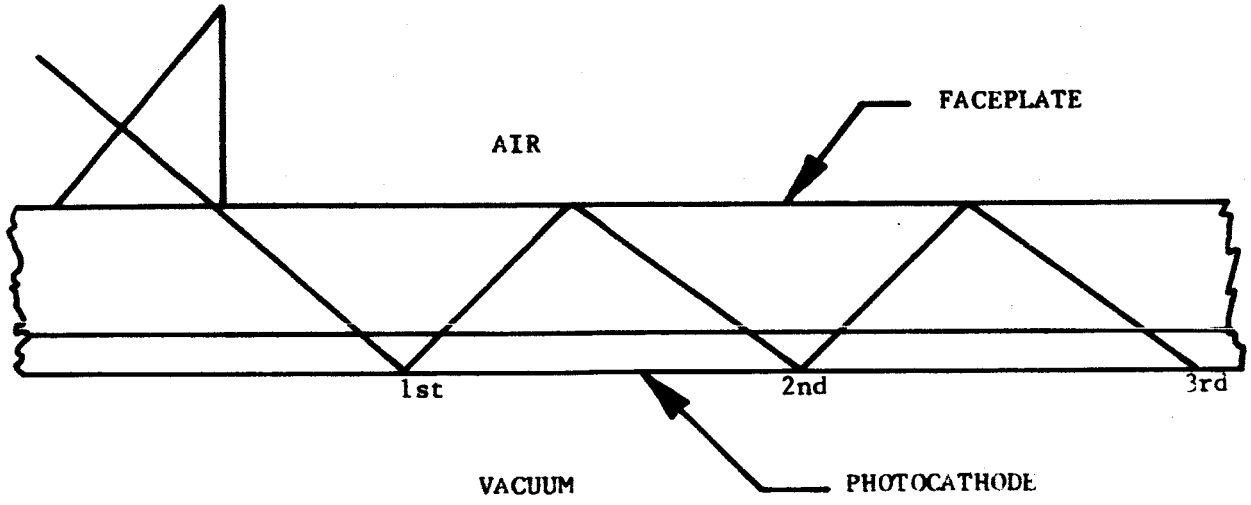

Figure 15

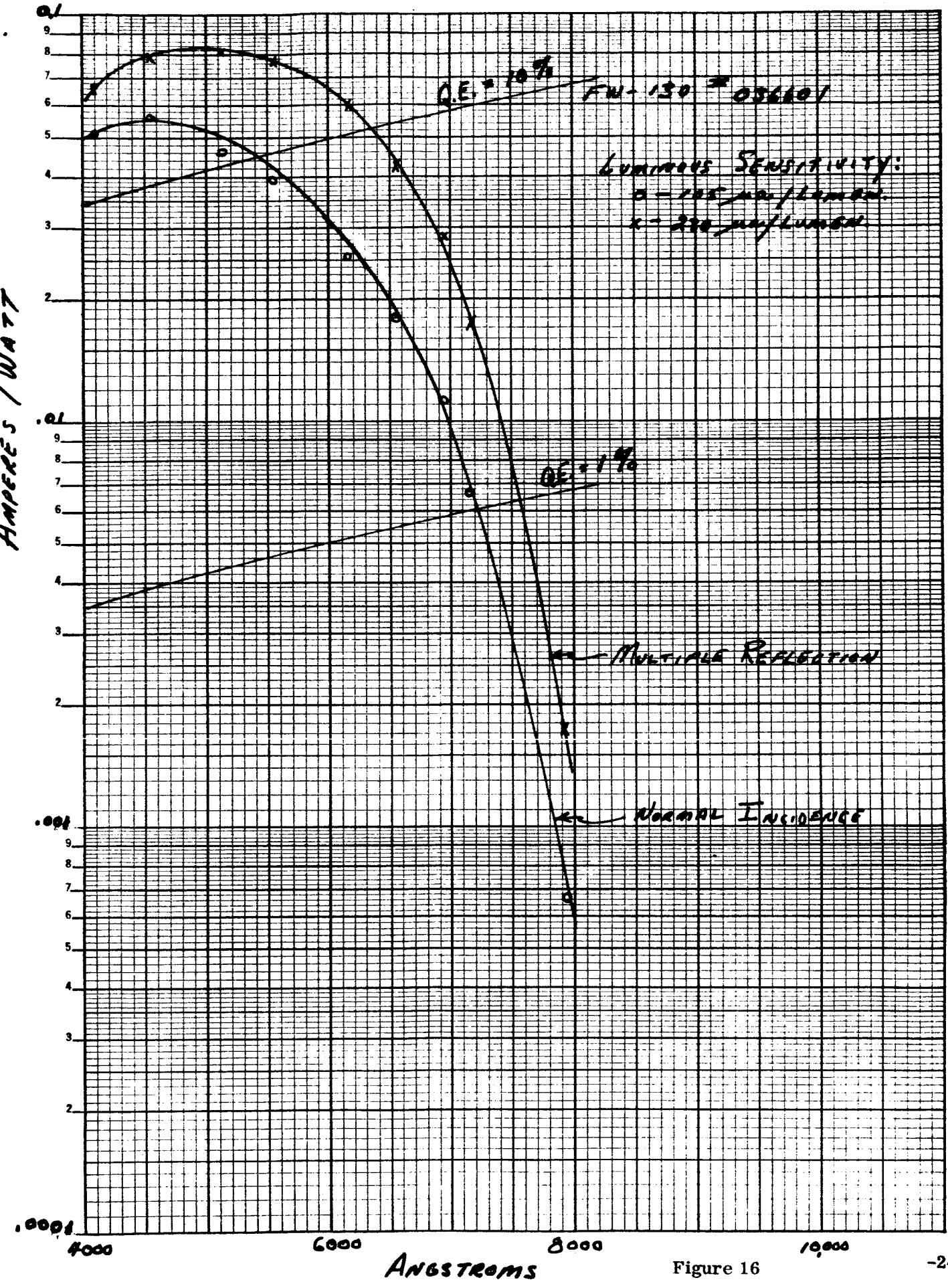
Amperes / Watt
.01
.001
.0001
Q.E. = 10%
FW-130 # 056601
Luminous Sensitivity:
o - 195 μa/Lumen
x - 220 μa/Lumen
Q.E. = 1%
Multiple Reflection
Normal Incidence
4000
6000
8000
10,000
Angstroms

Figure 16

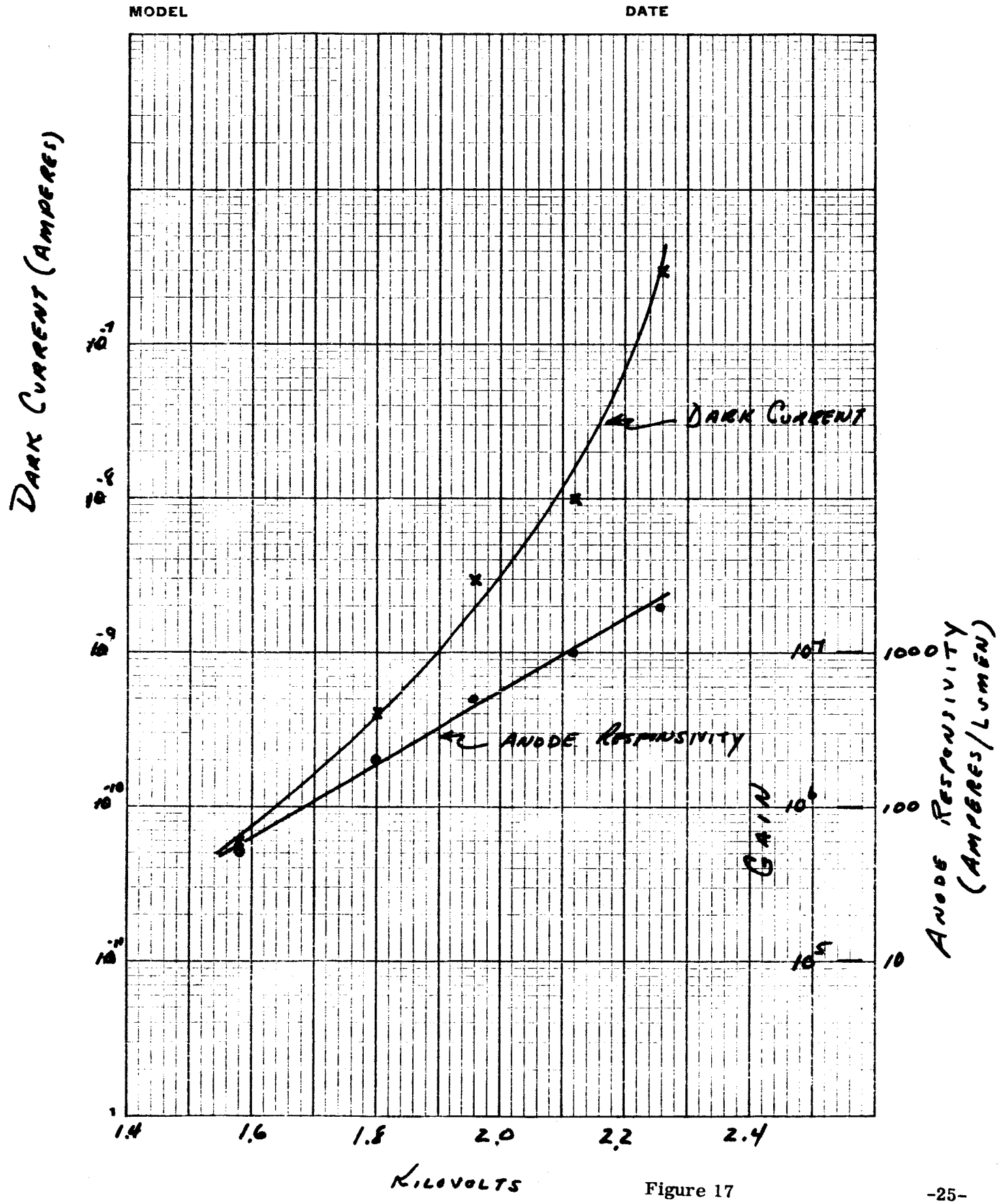
MODEL
DATE
DARK CURRENT (AMPERES)
DARK CURRENT
ANODE RESPONSIVITY
GAIN
ANODE RESPONSIVITY (AMPERES/LUMEN)
KILOVOLTS
1.4
1.6
1.8
2.0
2.2
2.4
1000
100
10
1

Figure 17

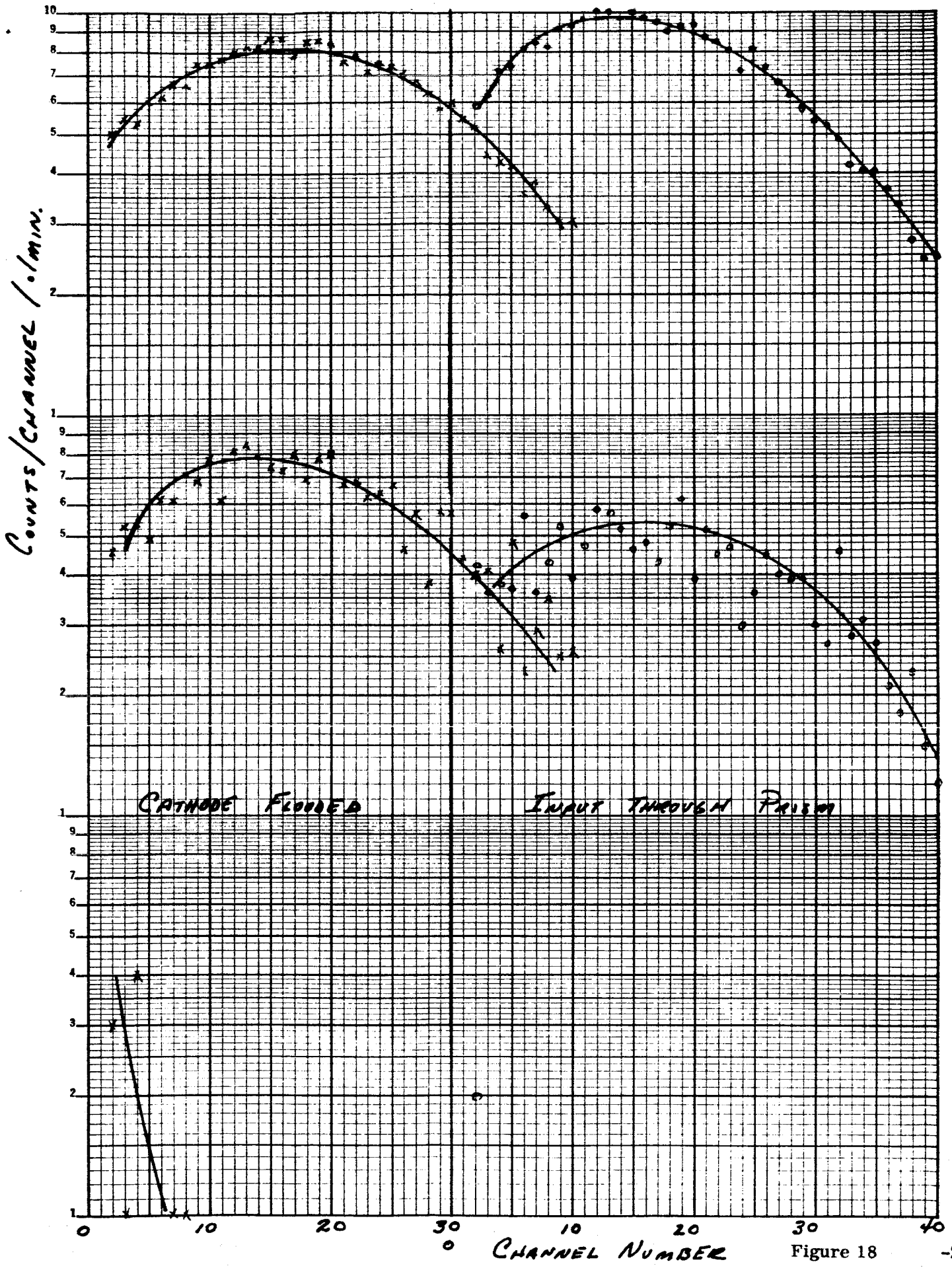
COUNTS/CHANNEL/MIN.
CATHODE FLOODED
INPUT THROUGH PRISM
CHANNEL NUMBER

Figure 18

(NASw 1038 Report)

APPENDIX I

MULTIPLE REFLECTION EFFECTS OBSERVED FOR S-1, S-11, AND S-20 PHOTOCATHODES

J. L. Gumnick and C. D. Hollish

ITT Industrial Laboratories
Fort Wayne, Indiana

Summary

A simple optical model has been used to describe the influence of light trapping on the performance of photocathodes. The model is based on the assumption that light trapping occurs as a result of total internal reflection in the faceplate-photocathode structure. The analysis based on the model predicts that successive light photocathode interactions are related through a geometric progression, and the ratios of light intensities and photoelectric yields associated with successive light photocathode interactions are equal to the common ratio of the progression. Experiments on S-1, S-11, and S-20 type photocathodes tend to confirm three predictions based on the analysis: that the logarithm of the photocurrent for a specific interaction is a linear function of the number denoting the interaction; that successive photocurrents and light intensities have the same ratio denoted K, and that the ratio of the total photocurrent to that of the first interaction approaches $\frac{1}{1-K}$.

Introduction

In recent years several researchers[1,2] have reported enhancement of photoelectric yield from photocathodes by using internal reflection techniques to produce multiple passes of light through the photocathode in photomultiplier tubes. Although improvements obtained using these methods have been measured and discussed, little attention has been given to the mechanisms responsible for these effects. In the present work experimental results for S-1, S-11, and S-20 photocathode types are compared to predictions based on a simple optical model used to describe internal reflection effects observed in flat faceplates with photocathodes on them.

The method used in the experiments to be discussed is illustrated in Fig. 1. A prism was used to inject light into a parallel plane faceplate with a photocathode deposited on it. Light was brought in at an angle O with the faceplate normal, and perpendicular to the prism. It interacted at the photocathode and returned to the air interface. At P the light was reflected back to the photocathode for a second interaction and so forth. In some experiments the light was permitted to escape after the first and second interactions by placing another prism of the same kind, but reversed in orientation at points P and Q in Fig. 1.

It can easily be shown that light traveling into the faceplate at an angle exceeding the critical angle for the faceplate-air interface will strike the photocathode-vacuum interface at an angle exceeding the critical angle for that interface. This is a consequence of refraction at the photocathode-faceplate interface. In this work all experiments were done with light incident at angles exceeding the critical angle and in the analysis internal reflections at the air and vacuum interfaces were assumed to be total.

Analysis

When light is let into the photocathode at an angle greater than the critical angle, the incident beam with an intensity I_1 strikes the photocathode-faceplate interface and is partially transmitted and partially reflected. The fraction transmitted will be called T and the fraction reflected R such that the sum of R and T equals unity. The intensity of the incident light that is reflected at the interface of the faceplate and photocathode will be called I_{1R} and it follows that:

$$I_{1R} = RI_1 \qquad (1)$$

A part of the incident beam will enter the photocathode. Assuming some absorption occurs in the photocathode, the beam will be attenuated, reflected at the photocathode-vacuum interface and attenuated still more before striking the faceplate-photocathode interface from the photocathode side. That intensity of the beam transmitted back through that interface will be called I^*_{1R} and can be expressed in terms of I_1 as:

$$I^*_{1R} = I_1 (AT)^2 \qquad (2)$$

In this equation A is one minus the fraction of light absorbed in a single pass through the photocathode. Since the angle of incidence is greater than the critical angle at the photocathode-vacuum interface, the reflection at that interface is unity. The above two terms can be grouped into a single expression:

$$I_2 = I_{1R} + I^*_{1R} = I_1\left[R + (AT)^2\right] \qquad (3)$$

This composite beam will strike the faceplate-air interface at P and be totally reflected back to the photo-

cathode. The beam leaving the photocathode-faceplate interface at the second interaction will be:

$$I_3 = I_{2R} + I^*_{2R} = I_1 \left[R + (AT)^2\right]^2 \quad (4)$$

Expressing successive terms as a function of I_1 gives for the Nth interaction:

$$I_N = I_1 \left[R + (AT)^2\right]^{N-1} \quad (5)$$

in which N is a positive integer denoting the number of the light-photocathode interaction. This equation describes the influence that reflections and absorption associated with the photocathode have on light trapped in the structure. In the development of the equation, for simplicity the ray reflected back into the photocathode at the photocathode-faceplate interface after being reflected at the vacuum interface is omitted as are higher order terms.

If the photocathode is uniform and homogeneous in its optical and electronic properties the photoelectric current from each spot of interaction can be written as:

$$i_N = SI_N \quad (6)$$

where i_N is the photoelectric current from spot numbered N and S is the photoelectric sensitivity of the photocathode. Dimensionally i_N will be in amperes when I is in watts and S is in amperes per watt. Introducing terms from the expression for I_N gives

$$i_N = SI_1 \left[R + (AT)^2\right]^{N-1} = i_1 \left[R + (AT)^2\right]^{N-1} \quad (7)$$

which is an expression for the photoelectric current from successive bounces of light trapped in an internally reflecting plane parallel structure. If the quantity $R + (AT)^2$ is defined to be K then

$$i_N = i_1 K^{N-1} \text{ and } I_N = I_1 K^{N-1} \quad (8a, b)$$

The factor K^{N-1} is the general term of a geometrical progression. The sum to infinity of such a progression is:

$$\sum_{N=1}^{\infty} K^{N-1} = \frac{1}{1-K} \quad (9)$$

An improvement factor F can be defined as the ratio of the net photocurrent for an infinite number of bounces i_T to that for the first bounce. It follows from Eq. 9 that

$$F = \frac{i_T}{i_1} = \frac{1}{1-K} \quad (10)$$

The ratio of successive terms for either the photoelectric current or the light intensity is:

$$\frac{i_N}{i_{N-1}} = \frac{I_N}{I_{N-1}} = \frac{K^{N-1}}{K^{N-2}} = K \quad (11)$$

From this treatment of multiple reflections three predictions can be made. The first is that a plot of the logarithm of the photoelectric current for successive bounces will be a linear function of N-1 since:

$$i_N = i_1 K^{N-1} \quad (12)$$

hence:

$$\ln i_N = \ln i_1 + (N-1) \ln K \quad (13)$$

The second is that successive light intensities or successive photoelectric currents observed for a given photocathode should have the same ratio which equals K. The third prediction is that the total measured photocurrent i_T in a multiple bounce experiment should approach in value $\frac{1}{1-K}$ times the photocurrent measured for the first interaction.

Values of K as a function of R for selected A values are plotted in Fig. 2. In Fig. 3 the factor $\frac{1}{1-K}$ is plotted as a function of K to illustrate the range of improvement factors that can occur for specific K values. If terms additional to those considered in Eqs. 3, 4, and 5 are included in the analysis, the result will be that K will be a more complicated function of T, A, and R than illustrated in Fig. 2. The other results discussed will be unchanged.

Experimental Results

Experiments to test the above three predictions were carried out on two types of tubes: image dissectors and diodes. Both tube types were made with faceplates of parallel plane type with photocathodes formed on the faceplate. In all cases light was admitted into the structure as described in Fig. 1. In the image dissector white light and filtered light at 7060 A° were used. For the diodes, laser light at 6328 A° was used.

Photocurrent Measurements for Successive Light-Photocathode Interactions

The image dissector[3] is a deflectable multiplier tube in which it is possible to displace an electronic image of a photocathode across the aperture of an electron multiplier chain. With this tube the photoelectric current from various parts of the photocathode can be measured separately. In this way photocurrents from successive light-photocathode interactions described above were measured. Details about the use of the image dissector in this type of study are reported elsewhere.[4]

Image dissector experiments were carried out with S-1, S-11, and S-20 type photocathodes. Typical data obtained in these experiments are plotted in Fig. 4. The logarithm of the peak photoelectric current at each region of the photoemission is plotted on the vertical scale and the interaction or bounce number, called

peak number on the figure is plotted on the horizontal scale as suggested by Eq. 13. All of the data taken on each of the three photocathodes with white light and at eight wavelengths between 4860 A° and 7060 A° were of the functional form of Eq. 13 as shown in Fig. 4. Slopes varied with wavelength and photocathode type.

Light Intensity Ratios and Photocurrent Ratios

According to Eq. 11 the ratio of photoelectric currents for successive interactions will be in the same ratio as measured light intensities. With the image dissectors and diodes the ratio of optical intensities were measured by determining the intensity of initial beam I_1 from the source and measuring I_2 by placing a prism at point P in Fig. 1 permitting I_2 to escape and be measured. Photoconductors and photoemitters were used to measure I_2 and I_1. The ratios were corrected for reflections at the prisms. The corrected measured ratios were called K_{OPT}.

Using the image dissector the values of successive peak photocurrents were measured and ratios calculated. In the diodes ratios were obtained by measuring the contribution of the first pass with an ejecting prism at P and the sum of the first and second pass contributions with an ejecting prism at point Q. The difference in photocurrents measured in this way was a measure of the photoelectric current at the second interaction. From these measurements ratios were calculated. The measured ratios of photocurrents for dissectors and diodes were called K_{PE}.

From Eq. 11 values of K_{OPT} and K_{PE} for any given photocathode are predicted to be equal. In Fig. 5 measurements of K_{OPT} and K_{PE} are plotted against each other. The data represent three photocathode types in six different vacuum tubes of two different types under three kinds of illumination. The data scatter around the line of predicted performance which is a straight line at 45°.

The results shown in Fig. 5 illustrate the range in values for K for different photocathodes with different types of illumination. These are not random, but are a manifestation of the fact that K is a function of R, A, and T, and different types of photocathodes show a wide range of these values, not only from type to type, but from photocathode to photocathode. These properties are also strongly wavelength dependent.

Ranges of Improvement Factors

While conducting these experiments, the total photocurrent was measured during the production of as many bounces as could be contained in a given faceplate. The total measured currents were denoted i^*_T. Using i^*_T together with the measured first bounce photocurrent i^*_1, a gain or improvement factor F* was determined for the experiments that are summarized in Fig. 5. These measured improvement factors F* were compared to calculated improvements based on the ranges of K in Fig. 5 using Eq. 10. The results are summarized in Table I.

Table I
Comparison of Ranges for Calculated and Measured Improvement Factors

		Calculated F	Measured F*
S-1	Max	2.0	1.7
	Min	1.5	1.3
S-11	Max	5.0	2.0
	Min	1.3	1.3
S-20	Max	3.5	3.3
	Min	2.5	2.0

S-1 Type Photocathodes For the S-1 photocathodes studied, from Fig. 3 and Fig. 5 predicted improvements F ranged between 1.5 and 2.0. The measured F* were between 1.3 and 1.7. The predicted values are slightly higher which is to be expected since the value F is based on an infinite number of bounces while the F* are for 4 to 8 bounces.

S-11 Type Photocathodes For S-11 types the range of F was between 1.3 to 5. In these experiments the range of F* was between 1.3 and about 2.0. Other workers[2] have reported improvements between 2.25 and 4.3 for S-11 type photocathodes.

S-20 Type Photocathodes For S-20 type photocathodes F were determined to be between 2.5 and 3.5. For F* values between 2.0 and 3.3 have been observed.

From Table I it can be seen that the predicted ranges of F based on experimental K values overlap the experimentally measured ranges of F*. Unfortunately, the data accumulated thus far is too sparse to permit more precise predictions of the general performance of photocathodes in the multiple bounce configuration.

Conclusions

The experimental results described tend to confirm the assumptions used in the analysis. However, the analytic description is not yet complete enough to predict the exact improvement expected for a specific photocathode in a particular multiple bounce experiment. Additional experiments are being carried out to relate specific ratio measurements to improvement factors. Moreover, work is being done to establish more exactly the functional relationship between the ratio of successive photocurrents and the optical characteristics of the photocathode being investigated.

Acknowledgment

The authors wish to thank Mr. K. R. Crowe for his assistance in several of the experiments and his contribution to many fruitful discussions.

References

1. Rambo, B. E., "Improved Long Wavelength Response of Photoemissive Surfaces," Air Force Tech. Rept. A1TDR-19, April (1964).

2. Gunter, W. D., Erickson, E. F. and Grant, G. R., Appl. Optics 4, 512 (1965).

3. Farnsworth, P. T., J. Franklin Inst. 218, 411 (1934).

4. Clayton, R. H. and Gumnick, J. L., Report on 25th Annual Conference on Physical Electronics, March 24-26, 1965, MIT, Cambridge, Mass.

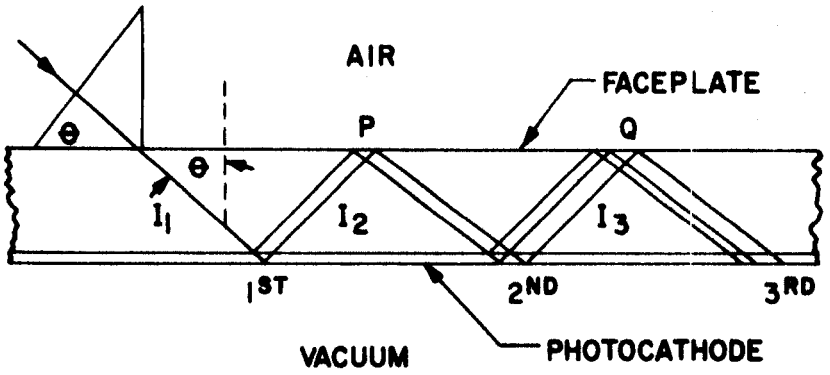

Figure 1. Schematic diagram of light paths during a multiple bounce experiment.

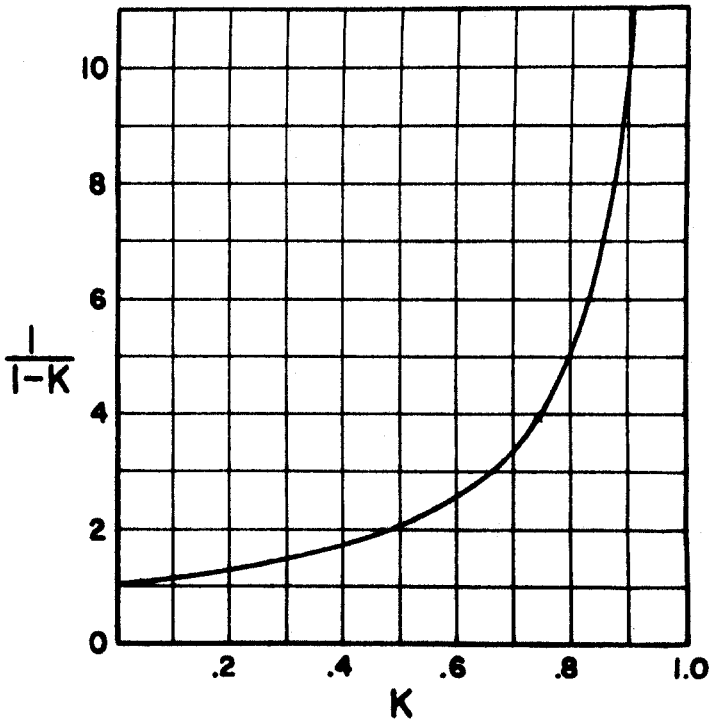

Figure 3. Graph of the enhancement factor $F=\frac{1}{1-K}$ versus ratio K.

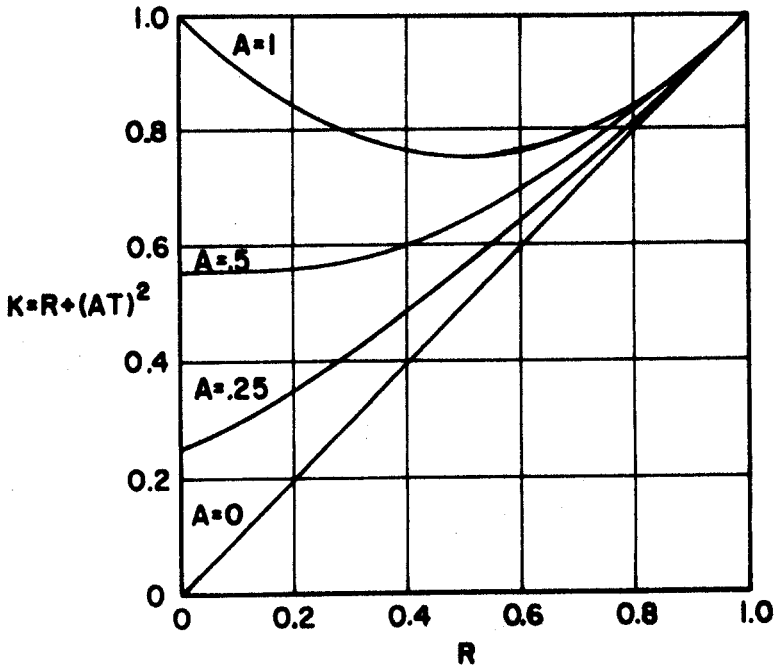

Figure 2. Graphs of the ratio K versus reflection R for selected A values.

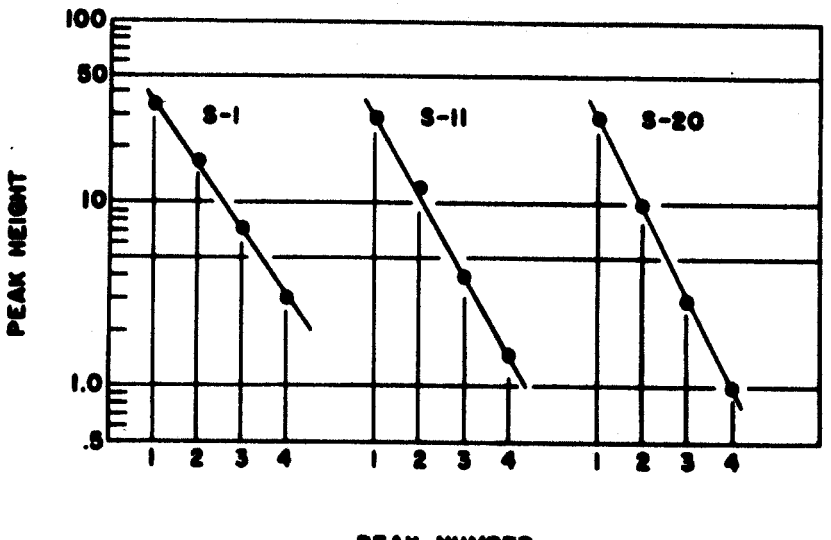

Figure 4. Photocurrent peak values in arbitrary units as a function of interaction number for S-1, S-11, and S-20 photocathode types.

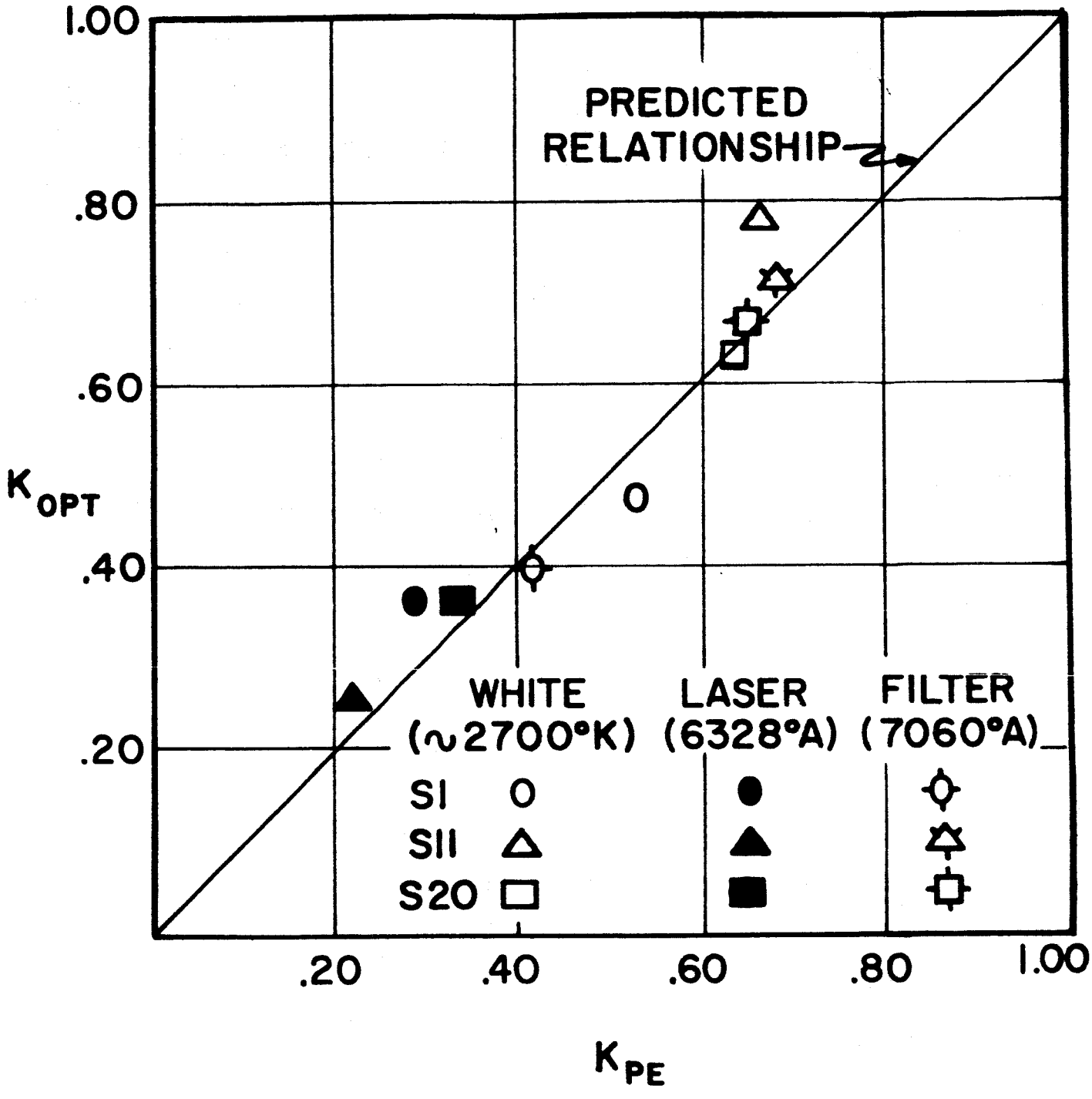

Figure 5. Experimentally measured light intensity ratios and photoelectric current ratios plotted together with a plot of the predicted relationship between them.